Anisotropic vortex pinning in the layered intermetallic superconductor CaAlSi

Ajay Kumar Ghosh,* Y. Hiraoka, M. Tokunaga, and T. Tamegai†
Department of Applied Physics, The University of Tokyo, 7-3-1 Hongo, Bunkyo-ku, Tokyo 113-8656, Japan
(Received 14 March 2003; published 3 October 2003)

We have studied anisotropic magnetic properties of layered intermetallic superconductor CaAlSi with moderate anisotropy. Near the upper critical field there is a prominent peak effect for $H||c$ at low temperatures and it becomes weaker for $H||ab$. The estimated correlation length L_c suggests the presence of three-dimensional collective pinning around the peak effect. The critical current densities for $H||c$ and $H||ab$ have been extracted and compared. Flux pinning mechanism in CaAlSi is anisotropic. Collective core pinning is observed for $H||c$ whereas there is a signature of deviation from it for $H||ab$. The vortex phase diagram, including the upper critical field, irreversibility field, and peak field, has been studied. The thermodynamic critical field and Ginzburg-Landau parameter have been estimated from the equilibrium magnetization. The nature of scaling of the maximum pinning force densities with the thermodynamic critical field has been discussed. The temperature dependence of London penetration depth is consistent with single fully gapped state in CaAlSi.

DOI: 10.1103/PhysRevB.68.134503 PACS number(s): 74.25.Op, 74.25.Qt, 74.70.Ad, 74.25.Ha

I. INTRODUCTION

The discovery of MgB_2 (Ref. 1) has been followed by several studies of the physical properties of hexagonal superconductors such as germanides[2] and silicides.[3,4] Among silicides with AlB_2 structure, so far CaAlSi is reported to be with the second highest critical temperature.[3] In this compound, several studies including the band-structure calculation have been reported, which reveal that both the honeycomb layer formed by Al and Si and the intercalated Ca layers control various superconducting properties.[3,5] However, not much work has been done on the mixed state and other related physical properties.

The mixed state properties of MgB_2 and related superconductors have been investigated by various groups recently to shed light on the several physical properties and their correlations.[6] Magnetization as a function of temperature and field has been studied to explore the possibilities of its applications. The magnetic hysteresis in MgB_2 has been studied by several groups. According to Larbalestier *et al.*, the linear behavior of the parameter $H^{0.25}\Delta M$ is reported to be valid within a broad range of temperature.[6] Studies of the magnetic moments of single crystalline MgB_2 lead to the extraction of various parameters which are found to be consistent with the standard Ginzburg-Landau (GL) and London models[7]. The hysteresis curves are analyzed on the basis of the scaling properties of magnetization at various temperatures, which reveal that irreversible magnetization of MgB_2 is dominated by the bulk pinning up to $T/T_c = 0.9$.[8] The critical current density for a pellet of MgB_2 is reported to be of the order of 10^5 A/cm^2 at 4.2 K,[9,10] which is high enough to apply it for technological applications. In a thin film of MgB_2, J_c is measured from M-H hysteresis and I-V curves and found to be 10^5 A/cm^2 at a magnetic field of 50 kOe at 15 K.[11] The analysis of J_c in MgB_2 from hysteresis shows that the pinning via the spatial fluctuation in critical temperature is important.[12]

Near the upper critical field, the temperature and magnetic-field dependent peak effect is another interesting feature of conventional superconductors such as Nb_3Ge,[13] 2H-$NbSe_2$,[14] and high-temperature superconductors including MgB_2.[15] Also, the study of the peak effect would be informative regarding the softening of vortices in these layered superconductors.

We have studied the hysteresis of magnetization of single crystalline CaAlSi for two field orientations with respect to the hexagonal honeycomb layers (*ab* plane). The peak effect has been studied along two directions. The anisotropic nature of the critical current density and the pinning force densities along two field orientations are evaluated and the possible mechanism of the pinning is discussed. The vortex phase diagram including irreversibility fields is determined. The London penetration depth is extracted from the equilibrium magnetization and the thermodynamic critical field.

II. EXPERIMENT

The ingots of CaAlSi prepared by arc-melting of 1:1:1 stoichiometric mixture of Ca, Al, and Si in Ar environment are used to prepare the feeding and seed rods for the floating-zone method to grow single crystals in Ar environment.[16] A single crystal with shiny surfaces from the boule is cut into rectangular shape with dimensions $3.0\times1.22\times0.95$ mm^3. We confirmed the reproducibility of data using other pieces of crystals. The magnetization M is measured by the superconducting quantum interference device magnetometer (Quantum Design MPMS) for the applied field in two directions with $H||c$ and $H\perp c$ in the temperature range between 2.0 K and 5.5 K.

III. RESULT AND DISCUSSIONS

The critical temperature of single crystalline CaAlSi is determined both from the magnetization at 5 Oe and zero-field resistivity measurements. The onset critical temperature is 6.0 K with a transition width of 0.2 K and the residual resistivity ratio of 2.7.[17]

The hysteresis curves at various temperatures are shown in Figs. 1(a) and 1(b) for $H||c$ and $H\perp c$, respectively. We show the hysteresis curves of CaAlSi at 2.0 K in the insets of

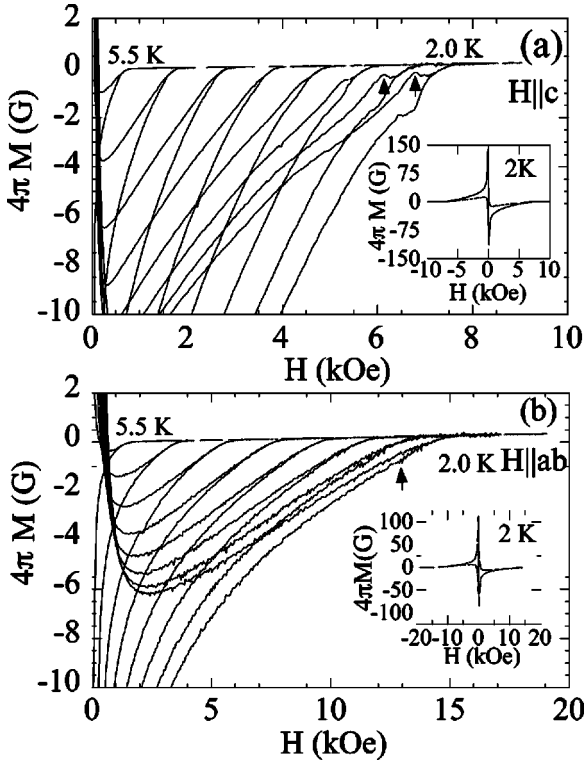

FIG. 1. Magnetization curves at various temperatures from 2.0 K to 5.5 K at an interval of 0.5 K for (a) $H||c$ and (b) $H||ab$. Arrows show some of the peak positions. Insets of (a) and (b) show the hysteresis curves at 2.0 K as representatives for $H||c$ and $H||ab$, respectively.

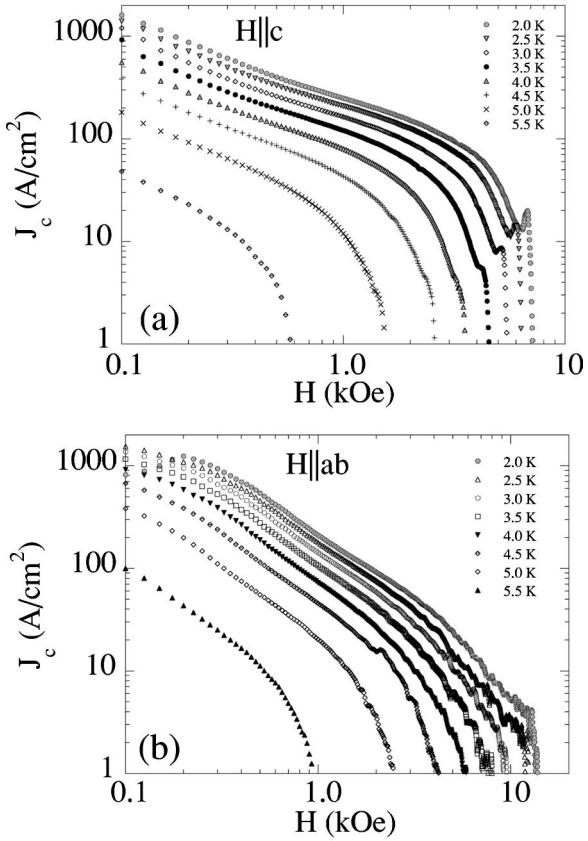

FIG. 2. Critical current density as a function of the applied field for (a) $H||c$ and (b) $H||ab$. In both cases the temperatures are between 2.0 K and 5.5 K with an interval of 0.5 K.

Figs. 1(a) and 1(b) for $H||c$ and $H\perp c$, respectively, as representatives of several temperatures. The M-H curves for $H||c$ show a sudden strong increase in magnetization at a certain field below the upper critical field as shown in Fig. 1(a). For $H||c$, the peak effect is very prominent at 2 K [see the arrows in Fig. 1(a)]. The height of the peak is reduced with increasing temperature and the peak in the magnetization becomes invisible above 4.5 K. The hysteresis curves for $H||ab$ shows weak signatures of peak effect only at low temperature as shown in Fig. 2(b) (see the arrow). Therefore, the peak effect is anisotropic in CaAlSi. It reflects the directional dependence of the pinning strength in CaAlSi.

The critical current densities J_c(A/cm^2) have been estimated using the relation of extended Bean model:[18,19]

$$J_c = \frac{40 M_{rem}}{b(1-b/3a)}. \tag{1}$$

Here, M_{rem}(emu/cm^3) is the irreversible magnetization and a (cm) and b (cm) are lateral dimensions of the sample ($a > b$). The variation of critical currents with field are shown in Figs. 2(a) and 2(b), for $H||c$ and $H||ab$, respectively. In case of $H||ab$ we have not discriminated between two different components of J_c flowing in the ab plane and along c axis. The critical current density in CaAlSi is smaller in order of magnitude in comparison to that in MgB_2.[9] Clearly, $J_c(H)$ for $H||c$ shows the peak effect close to the irreversibility field. As the temperature decreases the peak becomes prominent and shifts towards higher magnetic fields. It has been observed that MgB_2 follows small bundle pinning, particularly close to T_c, where J_c follows an exponential law:

$$J_c(H) = J_c(0)\exp[-(H/H_0)^{3/2}]. \tag{2}$$

Here, H_0 is a constant and $J_c(0)$ is the critical current density at zero field.[12] In CaAlSi, the variation of J_c does not fit with the above formula.

The peak effect has been observed in both low-T_c and high-T_c superconductors with a wide range of the anisotropic parameter. The occurrence of the peak effect in conventional superconductors was first discussed by Pippard.[20] Larkin and Ovchinnikov (LO) have explained the peak effect in critical current density near the upper critical field based on the softening of the flux lattice.[21] The concentration of pinning centers n and the correlation volume V_c, which displaces independently under the Lorentz force for a distance less than the coherence length, are very effective parameters to control the nature of the peak effect. According to LO formulations the peak effect disappears for the condition $f > a^2(\tilde{C}_{44}C_{66})^{1/2}$. Here, $\tilde{C}_{44} = C_{44}(1-H/H_{c2})\kappa^{-2}$ (κ: GL parameter), f is the force of interaction of individual pinning centers with vortex lattice, a is the vortex spacing, and C_{66} and C_{44} are shear and tilt elastic moduli, respectively. Therefore, the variation in the strength of the peak effect in CaAlSi is caused by the change in the ratio of pinning strength and the elastic energy.

Very strong peak effect in Nb_3Ge and anisotropic 2H-$NbSe_2$ around $0.9H_{c2}$ has been thoroughly studied.[13,14] The typical critical current density just below the peak effect in 2H-$NbSe_2$ is 1–30 A/cm^2 at 4.2 K and 10 kOe.[22] However, the peak effect in MgB_2, with strong pinning and current density, is also observed in the variation of real and imaginary parts of the ac susceptibility as functions of both magnetic field and temperature.[15] The peak effect in CaAlSi is more pronounced in comparison to that in MgB_2.[15] In addition, the borocarbide superconductors with a typical critical current density of 10 A/cm^2 at 3.0 K also shows peak effect.[23,24] In CaAlSi, the critical current density just below the peak effect is about 20–30 A/cm^2 for $H||c$ and 5–10 A/cm^2 for $H||ab$ at 4.0 K which is comparable to that in 2H-$NbSe_2$ and is much lower than of MgB_2. The peak effect in 2H-$NbSe_2$ is reported to be caused by the transition between the ordered and the disordered state of vortices.[25] However, magnetic decorations in $NbSe_2$ have shown that the enhancement of critical current density and the topology of the vortex structure are uncorrelated.[26] Therefore, the actual reason for the peak effect needs further studies.

The peak effect is controlled by several intrinsic parameters such as the product of number of pinning centers and correlation volume, elastic moduli, and the strength of pinning of individual centers. Following LO model we have the pinning force density $F_p = J_c B = (W/V_c)^{1/2}$. Here, W is the volume density of pinning centers and f the elementary pinning interaction. V_c is the correlation volume. Therefore, the change in $(W/V_c)^{1/2}$ is manifested in F_p around the peak effect region.[21] In CaAlSi, the lower critical current density and presence of the peak effect indicate that the strength of the individual pinning center is optimized with respect to the elastic energy which generates favorable condition for the peak effect. We have estimated the collective pinning length L_c using $L_c \sim \xi(J_0/J_c)^{1/2}$, where J_0 and J_c are the depairing critical current and critical current density, respectively, and ξ is the coherence length.[27] In the temperature and field region around peak effect, for example, at 4.2 K and 3 kOe, $J_0/J_c \sim 10^6$ and we estimate that L_c is about 4 ± 1 μm. The typical value of L_c for $NbSe_2$ in the peak effect region is ~ 10 μm.[28] A dimensional crossover is possible from two-dimensional to three-dimensional collective pinning when L_c becomes larger than the half of the sample thickness.[13] Around the peak effect in CaAlSi, L_c is smaller than the half of the thickness (~ 900 μm) of the sample. Therefore, three dimensional LO collective pinning describes the peak effect in CaAlSi.

In both $NbSe_2$ and YNi_2B_2C, the peak effect is observed for both $H||c$ and $H||ab$.[14,24] Also, in MgB_2 the peak effect is reported for both directions.[15,29] In anisotropic superconductors, shear moduli are different for different directions.[30] Accordingly, the strength of pinning has variation with direction, which is the major cause of the change in the strength of the peak effect for two directions. The angular dependence of the peak effect may be important in this compound, and it will be a future study.

Figure 3 shows the phase diagram of CaAlSi. The irreversibility field H_{irr} determined with the criterion of $J_c = 1$ A/cm^2 for both $H||c$ and $H||ab$ is also shown. The irreversibility fields show linear variation with temperature. The vortex phase diagram in Fig. 3 includes the upper critical fields H_{c2} for both $H||c$ and $H||ab$ obtained from the temperature dependence of magnetization at various fields.[16] The position of the peak effect, H_p, is also plotted in Fig. 3. H_p closely follows the temperature dependence of H_{c2} and it supports the softening of vortex lattice as its origin.

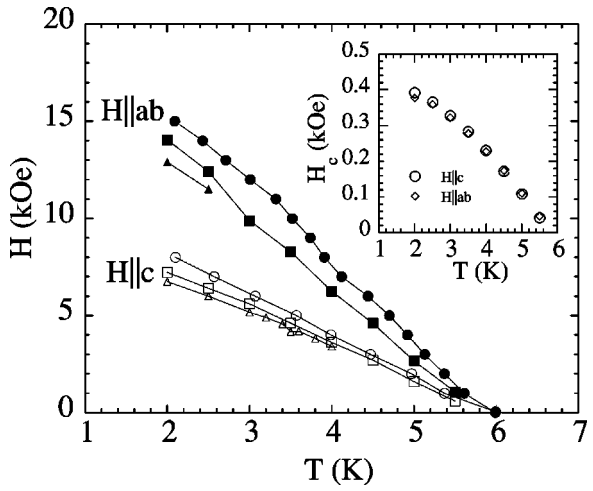

FIG. 3. Vortex phase diagram of CaAlSi. Solid circles and open circles represent H_{c2} for $H||ab$ and $H||c$, respectively [obtained from earlier $M(T)$ measurements]. Solid squares and open squares represent H_{irr} for $H||ab$ and $H||c$, respectively, obtained from $J_c(H)$ of the present study. Open and solid triangles correspond to the peak positions for $H||c$ and $H||ab$, respectively, at several temperatures. The solid lines through the data points are guide to eyes. Thermodynamical critical fields H_c at various temperatures for $H||c$ and $H||ab$ are shown in the inset.

We have extracted the pinning force density $F_p = J_c B$ and plotted in Figs. 4(a) and 4(b) as a function of applied field. In the inset of Figs. 4(a) and 4(b), $F_p/F_p(\max)$ is plotted with the reduced magnetic field H/H_{irr}. Though the scaling is observed at lower range of temperature, the global feature reveals that the scaling of pinning force density for $H||c$ is not present at higher temperature such as 5.5 K in CaAlSi. It suggests that the pinning mechanism is different at higher temperatures close to the transition temperature. However, the pinning scenario up to $T = 4.5$ K remains almost similar, including the peak effect.

It is noticeable that the variation of F_p for $H||ab$ is entirely different from that for $H||c$. In the latter case, F_p gradually decreases with the magnetic field and shows no broad peak as observed for $H||c$ [see Fig. 4(b)]. The pinning mechanism may be unaltered over a wide range of temperature from 2 K to 4.0 K. However, the scaling is not observed again at high temperatures above 4.5 K. Therefore, the pinning mechanism is more sensitive to temperature in the field orientation of $H||ab$. It clearly manifests the anisotropic pinning strength of individual centers with magnetic field. It will be interesting to mention that the pinning force density in nonmagnetic borocarbide is studied for $H||c$ and $H||ab$.[24] The magnitude and the nature of variation of $F_p(H)$ is found to be quite different for two directions. The possibility of other mechanisms besides nonlocal effects, which is gener-

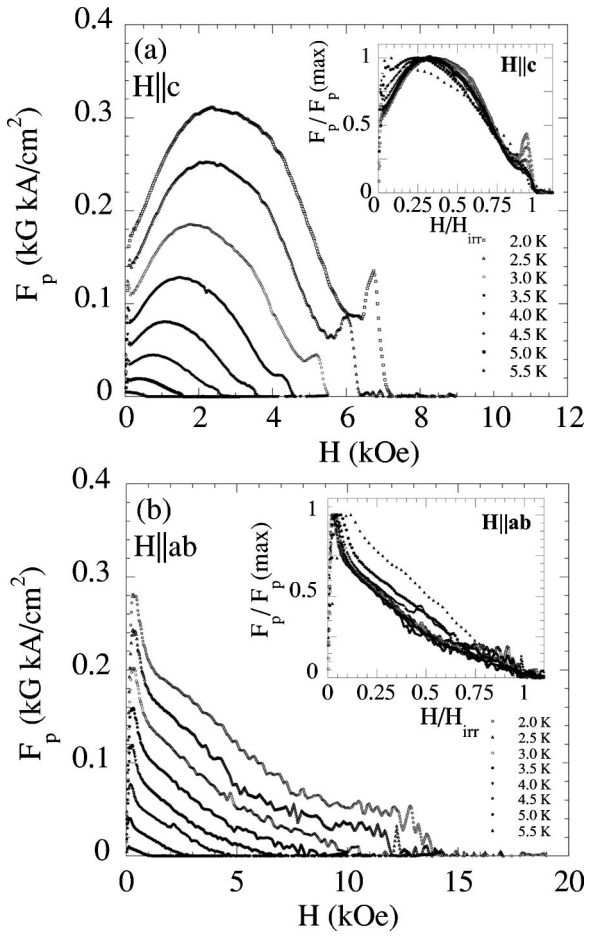

FIG. 4. Variations of pinning force density F_p with the magnetic field at various temperatures for (a) $H||c$ and (b) $H||ab$. Insets show the variation of F_p/F_p(max) with the reduced field H/H_{irr}. The scaling relation for each direction is found at lower temperatures.

ally observed for clean and high-κ superconductors, is attributed to the origin of the complexity of angular dependence of pinning force density.[24]

In the variation of F_p/F_p(max) with H/H_{irr} for $H||c$, the position of the peak indicates the nature of pinning. Peak positions at 0.4 to 0.5 demonstrate that the pinning centers are superconducting in nature with reduced order parameter. The F_p/F_p(max) versus H/H_{irr} for $H||c$ in CaAlSi shows a peak around $H/H_{irr}\sim 0.3$ [see inset of Fig. 4(a)] for $H||c$. According to the previous studies on the low-T_c superconductors, it will be at 0.33, which represents that the core pinning is responsible for such variation of the critical current density for $H||c$.[31,32] With the change in the field orientation, the peak positions is shifted towards 0.1, indicating deviation from the collective core pinning.

We have evaluated the equilibrium magnetization using $M_{eq}=(M_+ + M_-)/2$ for all temperatures where M_+ and M_- are magnetizations for increasing and decreasing field, respectively. Following the procedure shown by Thompson *et al.* for borocarbide superconductors[33] we have evaluated the reversible magnetizations. The reversible magnetization as a function of field for $H||c$ and $H||ab$ at various temperatures is shown in Figs. 5(a) and 5(b), respectively. Integrating the area under these curves we extract the thermodynamic critical field H_c and plot it in the inset of Fig. 3. We have assumed that the linear M_{eq}-ln(H) relation can be extrapolated to lower-field range, where the large irreversibility does not allow an accurate estimation of M_{eq}. H_c values are almost the same for two directions, giving evidence for bulk nature of superconductivity which strongly supports our previous finding of cusplike angular dependence of H_{c2} near $H||ab$.[16] Using $H_c(T)=H_c(0)(1-t^2)$, $H_c(0)$ is evaluated as 0.45 kOe. With this value and $H_{c2}(0)=\sqrt{2}\kappa H_c(0)$, we have evaluated in-plane London penetration depth $\lambda_{ab}(0)=3140$ Å. Together with the coherence length of $\xi_{ab}(0)=196$ Å (Ref. 16) the GL parameter κ is evaluated as 20 for $H||c$.

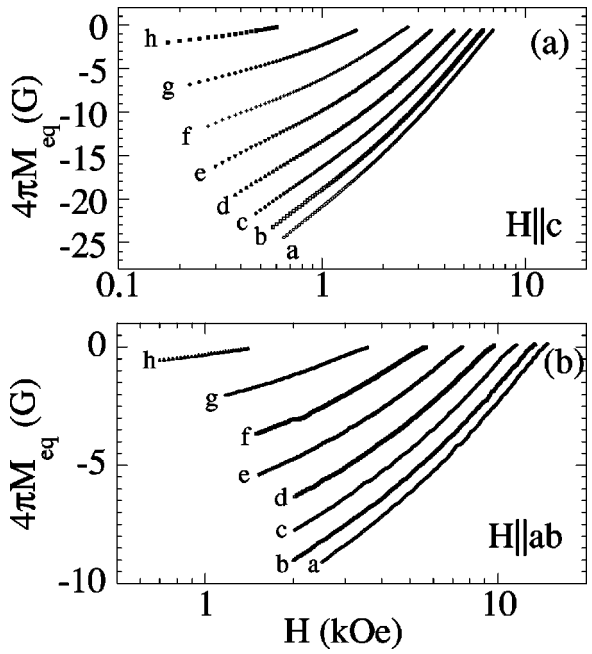

FIG. 5. Equilibrium magnetization with the magnetic fields for (a) $H||c$ and (b) $H||ab$ at various temperatures. (a)–(h) represent 2.0–5.5 K at an interval of 0.5 K in each panel.

The London penetration depth for $H||c$, λ_{ab}, can be independently obtained by using the London formula

$$-4\pi M=\frac{\alpha\Phi_0}{8\pi\lambda^2}\ln\left(\frac{\beta H_{c2}}{H}\right). \tag{3}$$

Here, Φ_0 is the flux quantum, and α and β are constants of the order of unity. In case of the core corrections in high-κ superconductor, α and β may differ from unity.[34,35] Using the slope of M_{eq} versus $\ln H$ in the region of $H_{c1}\ll H\ll H_{c2}$, and taking $\alpha=\beta=1$, we have extracted λ_{ab} as shown in Fig. 6. The variation of $\lambda_{ab}(T)$ is comparable to BCS model as shown in Fig. 6, whereas two-fluid model is not. The magnitude of the London penetration depth $\lambda_{ab}(0)=3100$ Å is consistent with that extracted using the thermodynamic critical field. This fact suggests that CaAlSi is a typical BCS superconductor with single fully opened gap.

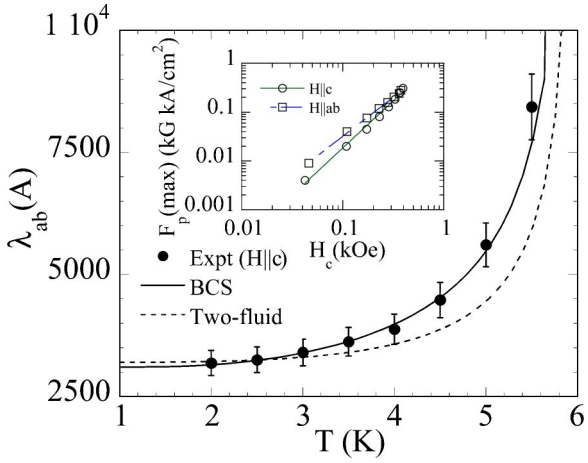

FIG. 6. London penetration depth λ_{ab} of CaAlSi as a function of temperature. The solid line and dotted lines represent BCS and Gorter-Casimir two-fluid models, respectively. Inset shows the variation of F_p(max) with H_c for $H||c$ and $H||ab$.

Scaling of pinning force density with the thermodynamical critical field provide the insight into the energy scale of the involved vortices.[36] We have plotted the maximum F_p for two directions with H_c in the inset of Fig. 6. F_p(max) is found to be scaled as $F_p \propto H_c^{\eta}$, where $\eta=2$ and 1.6 for $H||c$ and $H||ab$, respectively. It is interesting to mention that the exponent (η) for $LuNi_2B_2C$ is 2 for $H||ab$.[36] Since the line energy of vortex is proportional to H_c^2, it is reasonable to say that the lower value of η for $H||ab$ is correlated with the deviation from the collective core pinning.

Another interesting feature observed from the equilibrium magnetization is the nonlinear variation of M_{eq} with ln(H). The variation of the equilibrium magnetization with logarithmic magnetic field reveals that at lower temperatures the nonlinearity is prominent in both cases (see Fig. 5). As the temperature is increased to 5.5 K the variation of M_{eq} becomes linear for both field orientations. According to Kogan's formulation, high κ and clean materials show nonlinearity for the nonlocal corrections.[37] However, nonlinearity in M_{eq}-ln(H) curves in clean superconductor is in such a way that the slope $dM_{eq}/d\ln(H)$ decreases at higher fields. By contrast, the slope increases at higher fields in CaAlSi. This may correspond to the situation in $Lu(Ni_{0.91}Co_{0.09})_2B_2C$, where the crossover from the London to the linear regime shows up.[38]

IV. CONCLUSIONS

We have studied the magnetic hysteresis of single crystalline CaAlSi. The hysteresis of magnetization shows pronounced peak effect for $H||c$ and weak peak effect for $H||ab$. The observed peak effect is sensitive to the temperature. The collective correlation length for $H||c$ is about 4 ± 1 μm, indicating the three-dimensional collective pinning in the peak effect region of CaAlSi. The variation of critical current densities with field is anisotropic in nature. The scaling properties are observed for $H||c$, with an evidence of the collective core pinning. A different nature of scaling indicating rapid decrease in J_c with H is found for $H||ab$. The maximum pinning force densities for both directions scale with the thermodynamic critical field with exponent 2 and 1.6 for $H||c$ and $H||ab$, respectively. The in-plane London penetration depth obtained from equilibrium magnetization follows BCS-type temperature dependence, with $\lambda(0)$ $=3100$ Å, suggesting the presence of single fully opened gap.

ACKNOWLEDGMENTS

A.K.G. would like to acknowledge Japan Society for the Promotion of Sciences (JSPS) for support. This work was supported by a Grant-in-Aid for Scientific Research from the Ministry of Education, Culture, Sports, Science and Technology.

*Also at: Department of Physics, Jadavpur University, Kolkata 700032, India.

†Electronic address: tamegai@ap.t.u-tokyo.ac.jp

[1] J. Nagamatsu, N. Nakagawa, T. Muranaka, Y. Zenitani, and J. Akimitsu, Nature (London) **410**, 63 (2001).

[2] S. Majumdar and E.V. Sampathkumaran, Phys. Rev. B **63**, 172407 (2001).

[3] M. Imai, K. Nishida, T. Kimura, and H. Abe, Appl. Phys. Lett. **80**, 1019 (2002); M. Imai, E. Abe, J. Ye, K. Nishida, T. Kimura, K. Honma, H. Abe, and H. Kitazawa, Phys. Rev. Lett. **87**, 077003 (2001).

[4] T. Tamegai, A.K. Ghosh, Y. Hiraoka, and M. Tokunaga, Physica C (to be published); R.L. Meng, B. Lorenz, Y.S. Wang, J. Cmaidalka, Y.Y. Sun, Y.Y. Xue, J.K. Meen, and C.W. Chu, Physica C **382**, 113 (2002).

[5] I.R. Shein, V.V. Ivanovskaya, N.I. Medvedeva, and A.L. Ivanovskii, Pis'ma Zh. Eksp. Teor. Fiz. **76**, 223 (2002) [JETP Lett. **76**, 189 (2002)].

[6] D.C. Larbalestier, M.O. Rikel, L.D. Cooley, A.A. Polyanskii, J.Y. Jiang, S. Patnaik, X.Y. Cai, D.M. Feldmann, A. Gurevich, A.A. Squitieri, M.T. Naus, C.B. Eom, E.E. Hellstrom, R.J. Cava, K.A. Regan, N. Rogado, M.A. Hayward, T. He, J.S. Slusky, P. Khalifah, K. Inumaru, and M. Haas, Nature (London) **410**, 186 (2001).

[7] M. Zehetmayer, M. Eisterer, J. Jun, S.M. Kazakov, J. Karpinski, A. Wisniewski, and H.W. Weber, Phys. Rev. B **66**, 052505 (2002).

[8] M.S. Kim, C.U. Jung, M.S. Park, S.Y. Lee, K.H.P. Kim, W.N. Kang, and S.I. Lee, Phys. Rev. B **64**, 012511 (2001).

[9] D.K. Finnemore, J.E. Ostenson, S.L. Budko, G. Lapertot, and P.C. Canfield, Phys. Rev. Lett. **86**, 2420 (2001).

[10] P.C. Canfield, S.L. Budko, and D.K. Finnemore, Physica C **385**, 1 (2002).

[11] H.J. Kim, W.N. Kang, E.M. Choi, M.S. Kim, K.H.P. Kim, and S.I. Lee, Phys. Rev. Lett. **87**, 87002 (2001).

[12] M.J. Qin, X.L. Wang, H.K. Liu, and S.X. Dou, Phys. Rev. B **65**, 132508 (2002).

[13] R. Wordenweber, P.H. Kes, and C.C. Tsuei, Phys. Rev. B **33**, 3172 (1986).

[14] S. Bhattacharya and M.J. Higgins, Phys. Rev. Lett. **70**, 2617 (1993); Phys. Rev. B **49**, 10 005 (1994).
[15] M. Pissas, S. Lee, A. Yamamoto, and S. Tajima, Phys. Rev. Lett. **89**, 097002 (2002).
[16] A.K. Ghosh, M. Tokunaga, and T. Tamegai, Phys. Rev. B **68**, 054507 (2003).
[17] A.K. Ghosh, Y. Hiraoka, M. Tokunaga, and T. Tamegai, Physica C **392-396**, 29 (2003).
[18] C.P. Bean, Phys. Rev. Lett. **8**, 225 (1962).
[19] E.M. Gyorgy, R.B. Vandover, K.A. Jackson, L.F. Schneemeyer, and J.V. Waszczak, Appl. Phys. Lett. **55**, 283 (1989).
[20] A.B. Pippard, Philos. Mag. **19**, 217 (1967).
[21] A.I. Larkin and Yu.N. Ovchinnikov, J. Low Temp. Phys. **27**, 280 (1978); **34**, 409 (1979).
[22] M.J. Higgins and S. Bhattacharya, Physica C **257**, 232 (1996).
[23] K.J. Song, J.R. Thompson, M. Yethiraj, D.K. Christen, C.V. Tomy, and D.McK. Paul, Phys. Rev. B **59**, 6620 (1999).
[24] A.V. Silhanek, J.R. Thompson, L. Civale, D.McK. Paul, and C.V. Tomy, Phys. Rev. B **64**, 012512 (2001).
[25] Y. Paltiel, E. Zeldov, Y.N. Myasoedov, H. Shtrikman, S. Bhattacharya, M.J. Higgins, Z.L. Xiao, E.Y. Andrei, P.L. Gammel, and D.J. Bishop, Nature (London) **403**, 398 (2000).
[26] Y. Fasano, M. Menghini, F. de la Cruz, Y. Paltiel, Y. Myasoedov, E. Zeldov, M.J. Higgins, and S. Bhattacharya, Phys. Rev. B **66**, 020512 (2002).
[27] G. Blatter, M.V. Feigelman, V.B. Geshkenbein, A.I. Larkin, and V.M. Vinokur, Rev. Mod. Phys. **66**, 1125 (1994).
[28] K. Ghosh, S. Ramakrishnan, A.K. Grover, G.I. Menon, G. Chandra, T.V.C. Rao, G. Ravikumar, P.K. Mishra, V.C. Sahni, C.V. Tomy, G. Balakrishnan, D.Mck. Paul, and S. Bhattacharya, Phys. Rev. Lett. **76**, 4600 (1996).
[29] L. Lyard, P. Samuely, P. Szabo, T. Klein, C. Marcenat, L. Paulius, K.H.P. Kim, C.U. Jung, H.-S. Lee, B. Kang, S. Choi, S.-I. Lee, J. Marcus, S. Blanchard, A.G.M. Jansen, U. Welp, G. Karapetrov, and W.K. Kwok, Phys. Rev. B **66**, 180502 (2002).
[30] V.G. Kogan and L.J. Campbell, Phys. Rev. Lett. **62**, 1552 (1989).
[31] E.J. Kramer, J. Appl. Phys. **44**, 1360 (1973).
[32] D. Dew-Hughes, Philos. Mag. **30**, 293 (1974).
[33] J.R. Thompson, A.V. Silhanek, L. Civale, K.J. Song, C.V. Tomy, and D.McK. Paul, Phys. Rev. B **64**, 024510 (2001).
[34] Z. Hao and J.R. Clem, Phys. Rev. Lett. **67**, 2371 (1991).
[35] A.E. Koshelev, Phys. Rev. B **50**, 506 (1994).
[36] K.A. Ziq, P.C. Canfield, J.E. Ostenson, and D.K. Finnemore, Phys. Rev. B **60**, 3603 (1999).
[37] V.G. Kogan, A. Gurevich, J.H. Cho, D.C. Johnston, M. Xu, J.R. Thompson, and A. Martynovich, Phys. Rev. B **54**, 12 386 (1996).
[38] V.G. Kogan, S.L. Budko, I.R. Fisher, and P.C. Canfield, Phys. Rev. B **62**, 9077 (2000).